Development and validation of an early diagnosis model for bone metastasis in non-small cell lung cancer based on serological characteristics of the bone metastasis mechanism

Xiaoyan Teng,[a] Kun Han,[b] Wei Jin,[a] Liru Ma,[a] Lirong Wei,[a] Daliu Min,[b] Libo Chen,[c,**] and Yuzhen Du[a,*]

[a]Department of Laboratory Medicine, Shanghai Sixth People's Hospital Affiliated to Shanghai Jiao Tong University School of Medicine, Shanghai 200233, China
[b]Department of Oncology, Shanghai Sixth People's Hospital Affiliated to Shanghai Jiao Tong University School of Medicine, Shanghai 200233, China
[c]Department of Nuclear Medicine, Shanghai Sixth People's Hospital Affiliated to Shanghai Jiao Tong University School of Medicine, Shanghai 200233, China

eClinicalMedicine 2024;72: 102617
Published Online xxx
https://doi.org/10.1016/j.eclinm.2024.102617

Summary

Background Bone metastasis significantly impact the prognosis of non-small cell lung cancer (NSCLC) patients, reducing their quality of life and shortening their survival. Currently, there are no effective tools for the diagnosis and risk assessment of early bone metastasis in NSCLC patients. This study employed machine learning to analyze serum indicators that are closely associated with bone metastasis, aiming to construct a model for the timely detection and prognostic evaluation of bone metastasis in NSCLC patients.

Methods The derivation cohort consisted of 664 individuals with stage IV NSCLC, diagnosed between 2015 and 2018. The variables considered in this study included age, sex, and 18 specific serum indicators that have been linked to the occurrence of bone metastasis in NSCLC. Variable selection used multivariate logistic regression analysis and Lasso regression analysis. Six machine learning methods were utilized to develop a bone metastasis diagnostic model, assessed with Area Under the Curve (AUC), Decision Curve Analysis (DCA), sensitivity, specificity, and validation cohorts. External validation used 113 NSCLC patients from the Medical Alliance (2019–2020). Furthermore, a prospective validation study was conducted on a cohort of 316 patients (2019–2020) who were devoid of bone metastasis, and followed-up for at least two years to assess the predictive capabilities of this model. The model's prognostic value was evaluated using Kaplan–Meier survival curves.

Findings Through variable selection, 11 serum indictors were identified as independent predictive factors for NSCLC bone metastasis. Six machine learning models were developed using age, sex, and these serum indicators. A random forest (RF) model demonstrated strong performance during the training and internal validation cohorts, achieving an AUC of 0.98 (95% CI 0.95–0.99) for internal validation. External validation further confirmed the RF model's effectiveness, yielding an AUC of 0.97 (95% CI 0.94–0.99). The calibration curves demonstrated a high level of concordance between the anticipated risk and the observed risk of the RF model. Prospective validation revealed that the RF model could predict the occurrence of bone metastasis approximately 10.27 ± 3.58 months in advance, according to the results of the SPECT. An online computing platform (https://bonemetastasis.shinyapps.io/shiny_cls_1model/) for this RF model is publicly available and free-to-use by doctors and patients.

Interpretation This study innovatively employs age, gender, and 11 serological markers closely related to the mechanism of bone metastasis to construct an RF model, providing a reliable tool for the early screening and prognostic assessment of bone metastasis in NSCLC patients. However, as an exploratory study, the findings require further validation through large-scale, multicenter prospective studies.

Funding This work is supported by the National Natural Science Foundation of China (NO.81974315); Shanghai Municipal Science and Technology Commission Medical Innovation Research Project (NO.20Y11903300); Shanghai Municipal Health Commission Health Industry Clinical Research Youth Program (NO.20204Y034).

*Corresponding author.
**Corresponding author.
E-mail addresses: yzdu@sjtu.edu.cn (Y. Du), lbchen@sjtu.edu.cn (L. Chen).

Keywords: Bone metastasis; Early diagnosis; Machine learning; Model interpretability; Risk assessment

Research in context

Evidence before this study

A comprehensive search was conducted on PubMed for publications prior to February 27, 2024, utilizing search terms "Bone metastasis," "early diagnosis," and "machine learning," without language restrictions. The search yielded a limited number of relevant studies. Although there have been studies on early diagnosis of tumor bone metastasis, no diagnostic model for bone metastasis in non-small cell lung cancer (NSCLC) patients has been established.

Added value of this study

In this study, machine learning algorithms were employed to develop a diagnostic model for bone metastasis in NSCLC, utilizing data from 664 patients with primary stage IV NSCLC who had received a pathological diagnosis. The Random Forest (RF) model, which includes age, sex, and 11 serum molecular features, demonstrated the highest accuracy. The area under the receiver operating characteristic curve (AUC) of the RF model was 0.98 (95% CI 0.95–0.99) and 0.97 (95% CI 0.94–0.99) in the internal and external validation cohorts, respectively. Prospective validation revealed that, regarding the results of the SPECT, the RF model—which consists of clinical and plasma biomarkers, can diagnose bone metastasis non-invasively yet reliably. Additionally, the RF model can predict the occurrence of bone metastasis approximately 10.27 ± 3.58 months in advance.

Implications of all the available evidence

The RF model established in our study has the potential to be a valuable diagnostic tool for early detection and progression monitoring of bone metastasis in NSCLC patients. The results of this study enable early prediction of bone metastasis, providing a basis for early intervention, reducing the incidence of skeletal-related events (SREs), and ultimately supporting the improvement of the quality of life of cancer patients and contributing to the management of cancer as a chronic condition. To facilitate the use of the RF model, a free online computing platform has been made available at: https://bonemetastasis.shinyapps.io/shiny_cls_1model/. This platform offers doctors and patients a free online tool for early diagnosis of NSCLC bone metastasis and prognosis assessment, benefiting a wider range of patients.

Introduction

Lung cancer ranks among the most prevalent cancers globally, characterized by high incidence and mortality rates.[1] Notably, non-small cell lung cancer (NSCLC) constitutes approximately 85% of all lung cancer cases.[2] A significant proportion of NSCLC patients, between 26% and 36%, develop bone metastasis.[2] Studies have shown that the median survival duration for NSCLC patients after developing bone metastasis ranges from 5 to 11.5 months.[3,4] The bone destruction associated with metastasis can lead to skeletal-related events (SREs), such as bone pain, fractures, spinal cord compression, and hypercalcemia, significantly affecting patients' survival and quality of life.[5] Therefore, the prompt identification, diagnosis, and management of bone metastasis in NSCLC are crucial for improving patient outcomes and quality of life.

Currently, the primary clinical approach for diagnosing tumor bone metastasis relies on imaging techniques.[6] However, these methods have limited sensitivity, resulting in a delayed diagnosis and exposure to radiation.[7] Imaging is also unsuitable for frequent disease monitoring. Furthermore, the National Comprehensive Cancer Network (NCCN) screening guidelines in the United States similarly discourage imaging assessments for asymptomatic patients.[8,9] Consequently, there is a pressing need for an effective and easily accessible tool for the early diagnosis and risk assessment of NSCLC bone metastasis.

The occurrence of bone metastasis is a dynamic process,[10,11] which is closely associated with the interaction of cell factors derived from bone microenvironment and the imbalance of regulatory factors derived from bone metabolism.[12,13] Simultaneously, bone metastasis disrupt the balance between bone resorption and formation, leading to the release of a series of products related to bone metabolism into the bloodstream.[12,14] Literature reports suggest that changes in these factors in the serum may precede the detection of bone metastasis through imaging.[15] However, due to the complexity and diversity of these indicators, the sensitivity and specificity of individual indicators are limited. Therefore, it is essential to comprehensively consider multiple factors to thoroughly explore their diagnostic utility in tumor bone metastasis.

The objective of this study was to develop an early diagnostic model for bone metastasis by examining serum indicators closely associated with the mechanisms of bone metastasis. Candidate indicators included regulators of calcium and phosphorus metabolism (Ca, P, PTH, CT), bone turnover markers (BAP, tP1NP, OPG, NMID, β-CTx), bone-related hormones and cytokines (FT3, FT4, TSH, IL-6, PTHRP), and electrolytes (K, Na, Mg, Cl). The modeling approach utilized six

distinct machine learning algorithms, namely decision tree (DT), logistic regression (Logistic), multilayer perceptron (MLP), random forest (RF), support vector machine (SVM), and extreme gradient boosting (Xgboost), to construct the model.[16] Through internal validation, external validation, and prospective validation, the efficacy of various algorithmic models was compared, and their predictive capacity was evaluated to identify the most optimal model. Finally, an online computing platform based on the optimal model was developed to facilitate the early diagnosis and prognostic assessment of bone metastasis in NSCLC patients.

Methods

Research design

The research design for this study is depicted in Fig. 1 and comprises of 5 steps: development, internal validation, external validation, prospective validation, and interpretation. Initially, a training cohort, constituting 70% of the derivation cohort, was used to develop predictive models. Subsequently, the remaining 30% of the derivation cohort was designed for internal validation, while an independent validation dataset was employed for external validation. Furthermore, a follow-up study with a minimum duration of two years was conducted using a prospective validation cohort. Regarding the results of the Single Photon Emission Computed Tomography (SPECT), the model's performance was evaluated. The Shapley Additive explanations (SHAP) algorithm was utilized to elucidate the significance of features in the predictive model and to identify nonlinear relationships among risk predictors.

Study subjects

The derivation cohort, external validation cohort, and prospective validation cohort adhered to the same inclusion and exclusion criteria. Inclusion criteria were as follows: a. Patients diagnosed with stage IV NSCLC; b. Patients who underwent Single Photon Emission Computed Tomography (SPECT) during hospitalization to diagnose bone metastasis and also received Magnetic Resonance Imaging (MRI) examinations of suspicious areas; c. Patients without severe diseases affecting the heart, lungs, liver, kidneys, or blood system; d. Patients aged between 40 and 80 years old, with a maximum age difference of ≤20 years within the same cohort, including both males and females; e. Patients whose weight was within ±10% of standard weight; f. Patients who signed an informed consent form. The exclusion

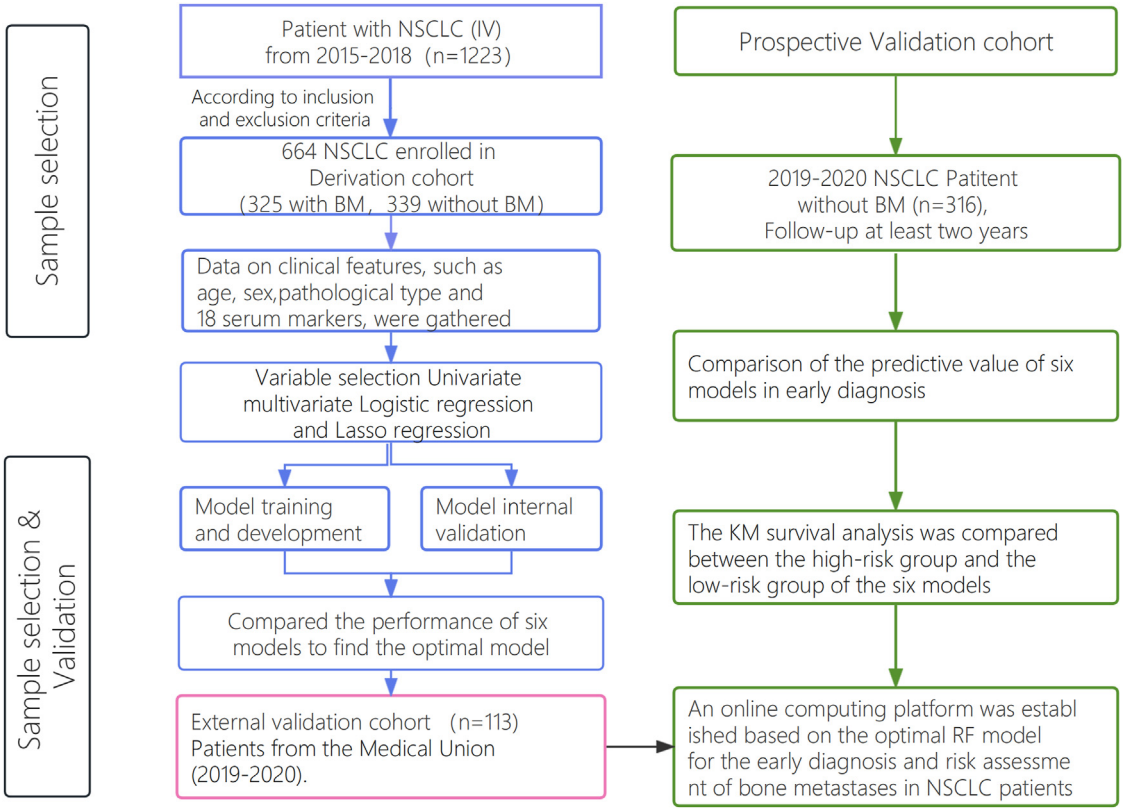

Fig. 1: Flow diagram of the study population. Abbreviations: BM: bone metastasis; NBM: none-bone metastasis; NSCLC: Non-Small Cell Lung Cancer.

criteria were as follows: a. Patients with a history of traumatic fractures prior to enrollment; b. Patients with endocrine diseases affecting bone metabolism; c. Patients diagnosed with other malignant tumors or those with abnormal liver function; d. Patients who had used medications affecting bone metabolism, such as bisphosphonates or denosumab, within the past 3 months; e. Pregnant and lactating women. According to the "Expert Consensus on the Diagnosis and Treatment of Bone metastasis in Lung Cancer (2019 Version)"[17] all patients underwent screening undergo SPECT for screening for bone metastasis. The frequency of bone SPECT imaging was determined by clinic doctor and did not exceed 6 months.

The derivation cohort included patients treated at our hospital from January 2015 to December 2018, diagnosed with primary stage IV NSCLC. A total of 1223 individuals meeting these criteria were screened for participation. Based on the exclusion criteria, 317 patients had undergone various treatments such as chemotherapy, radiation therapy, immunotherapy, bisphosphonate therapy, or other therapies within the three months prior to their inclusion. Additionally, 205 patients had been diagnosed with endocrine, immune, or metabolic disorders, while 37 patients had incomplete or missing data. Consequently, a total of 664 eligible patients were selected for the derivation cohort. Among these patients, 325 were diagnosed with bone metastasis based on bone SPECT imaging and MRI examinations of suspicious areas, forming the bone metastasis group. The remaining 339 patients showed no signs of bone metastasis based on bone SPECT imaging and MRI examinations of suspicious areas, constituting the non-bone metastasis group. Supplementary Table S1 presents an overview of the clinical characteristics of the 664 patients included in the derivation cohort.

The external validation cohort consisted of 113 eligible NSCLC patients, recruited from the Sixth People's Hospital Medical Alliance between January 2019 and December 2020. Among these, 46 patients (40.71%) had bone metastasis, while 67 patients did not. In terms of baseline clinical characteristics, such as age and sex, the derivation and external validation cohorts exhibited similarities. Supplementary Table S1 presents an overview of the clinical characteristics of the 113 patients included in the external validation cohort.

The prospective validation cohort consisted of 316 patients selected from the Sixth People's Hospital between January 2019 and December 2020. These patients were initially diagnosed with stage IV primary NSCLC without bone metastasis during their initial hospitalization. Subsequently, patients were subjected to continuous monitoring until December 2022, ensuring a minimum follow-up duration of two years. To monitor the development of bone metastasis, all patients underwent bone SPECT every 3–6 months. The clinical characteristics of the 316 patients included in the prospective validation cohort are outlined in Supplementary Table S1.

Data collection

This study collected patient data on age, sex, and laboratory test results of tumor bone metastasis indicators by reviewing electronic medical records and the laboratory management system. The laboratory test results included various aspects such as regulation features of calcium-phosphorus metabolism (Ca, P, PTH, CT), bone turnover markers (BAP, tP1NP, OPG, N-MID, β-CTx), hormones and cytokines related to bone metabolism (FT3, FT4, TSH, IL-6, PTHRP), and electrolytes (K, Na, Mg, Cl). These variables were considered potential predictive factors. The full names and abbreviations of the included features are listed in Supplementary Table S2. In cases of missing data in the electronic medical records, this issue was addressed by conducting supplementary examinations on serum samples obtained from patients, which were stored in the laboratory sample repository.

Laboratory indicator measurements

Blood samples were collected from patients in the morning, on an empty stomach, before anticancer treatment on the first day of hospitalization. The samples were allowed to sit at room temperature for 30 min, then centrifuged at 3500×*g* for 10 min. The resultant serum was tested within 4 h while being stored at 4 °C, with any remaining serum stored at −80 °C.

The serum concentrations of tP1NP (03141071190), β-CTx (11972308122), and IL-6 (05109442190) were quantitatively determined using the Roche Diagnostics Cobas E601 (Switzerland) fully automated electrochemiluminescence immunoassay analyzer (ECLIA) and its original reagents. The intra-batch precision for tP1NP, β-CTx, and IL-6 was within 8.7%, 5.7%, and 5.1%, respectively, while the inter-batch precision did not exceed 3.2%, 4.7%, and 3.9%, respectively.

Serum levels of BAP, N-MID, TSH, PTH, CT, IL-6, FT4, and FT3 were quantitatively assessed using the Beckman Coulter DXI800 (USA) fully automated chemiluminescence immunoassay analyzer and its original reagents. Additionally, the serum concentrations of K, Na, Cl, Ca, P, and Mg were quantitatively measured using the Beckman Coulter AU5800 fully automated blood biochemical analyzer and its original reagents.

Serum concentrations of OPG (BYS10849B) and PTHRP (BYS10753B) were quantitatively measured using an enzyme-linked immunosorbent assay (ELISA) technique with a microplate reader (Biotech, Winooski, USA). The repeatability coefficient of variation (CV) for these assays was found to be below 15%.

Statistical analysis

Baseline data analysis of patients began with normality tests on the quantitative data. Normally distributed continuous data were presented as Mean ± SD, and comparisons between groups were conducted using independent samples t-tests. Skewed data were described using the median (P25, P75), with group comparisons performed via the Mann–Whitney U tests. Count data were expressed as frequency (percentage, %), with chi-square tests used for statistical analysis.

ROC curve analysis evaluated the diagnostic performance, using the optimal Youden index method to determine the cut-off values for each indicator. Multivariate logistic regression and Lasso regression analyses were then used to finalize the variables for inclusion, thereby eliminating any redundant features. Logistic regression identified independent risk factors for bone metastasis in NSCLC patients. Additionally, survival analysis utilized Kaplan–Meier survival curve, with differences assessed using the log-rank test. A two-tailed *P*-value of less than 0.05 was deemed statistically significant.

Variable selection

To determine the variables for inclusion in the machine learning models, a preliminary univariate analysis assessed differences in various indicators between patients with and without bone metastasis. Both univariate and multivariate analyses utilized binary logistic regression. Multivariate logistic regression analysis, applying variables with statistically significant differences in univariate analysis (α entry = 0.05, α exit = 0.1), estimated the odds ratio (OR) and the 95% confidence interval (CI) for the OR. A *P*-value of less than 0.05 was considered statistically significant. Lasso regression analysis, implementing the L1 regularization method, established inclusion and exclusion criteria based on the magnitude of coefficient variables. Lasso regression adds an L1 penalty term to the loss function, driving some coefficients to zero and thus enabling automatic feature selection. In the Independent variables with zero coefficients were excluded, while those with non-zero coefficients were retained in the Lasso regression.

Model derivation and validation

The machine learning algorithm models were developed using Python version 3.8 and R version 4.2.3, in conjunction with the Tidymodels package. Tidymodels is a suite of packages designed for machine learning, adhering to tidy principles. In this study, six machine learning algorithms—Decision Tree (DT), Logistic Regression (Logistic), Multilayer Perceptron (MLP), Extreme Gradient Boosting (Xgboost), Support Vector Machine (SVM), and Random Forest (RF)— were utilized to construct the bone metastasis diagnostic model via the Tidymodels package. The models were constructed as follows: The DT model using the decision_tree function, with the engine set to "rpart"; the MLP model using the mlp function with the engine set to "mlp"; the Xgboost model using the boost_tree function with the engine set to "xgboost"; the Logistic model using the logistic_reg function with the engine set to "glm"; the SVM model using the svm_rbf function with the engine set to "kernlab"; and the RF model using the rand_forest function with the engine set to "randomForest".

The derivation cohort was divided into a 70% training cohort and a 30% internal validation cohort. The development of the models employed six machine learning algorithms: Logistic, DT, MLP, RF, SVM, and Xgboost. Each classification algorithm underwent hyperparameter tuning through 5-fold cross-validation internally. After selecting the optimal hyperparameters, the model was retrained on the complete training subset to finalize the weighting and generate a locked model. These locked models were then assessed on the internal validation cohort. The evaluation of the trained models' performance included the comparing ROC curves and using the Wilcoxon signed-rank test to evaluate the model's adequacy. The efficacy of the six machine learning algorithms was assessed across the internal validation, external validation, and prospective validation cohorts. Ultimately, the most optimal model was utilized to develop an online computing platform.

Ethics statement

Ethical approval for this study was granted by the Ethics Review Committee of the Sixth People's Hospital affiliated to Shanghai Jiao Tong University School of Medicine (Approval No. 2019-019). All participants in the study were provided with information regarding the study's content and subsequently signed written informed consent.

Role of the funding source

The funding source had no role in the study design, data collection, analysis, interpretation of data, the writing of the report, or in the decision to submit the paper for publication. All authors had full access to all data in the study and had final responsibility for the decision to submit for publication.

Results

Patient characteristics

This study conducted an initial comparison among three study groups: the healthy control group (123 individuals), the non-bone metastasis group (339 patients), and the bone metastasis group (325 patients). The comparison focused on their baseline characteristics including age at first admission, sex, and the baseline levels of 18 serum indicators (Table 1).

In the comparison between the bone metastasis group and the non-bone metastasis group (BM vs.

Characteristics	Healthy control (n = 123)	NBM (n = 339)	BM (n = 325)	*P* value[a]	*P* value[b]	*P* value[c]
Sex (female)	55 (44.72%)	119 (35.10%)	127 (39.08%)	0.24	0.99	0.49
Age	62 (56–72)	64 (58–70)	64 (59–69)	0.31	0.14	0.090
Ca	2.3 (2.2–2.4)	2.23 (2.13–2.31)	2.28 (2.17–2.41)	<0.0001	<0.0001	0.0058
P	1.1 (1.0–1.3)	1.05 (0.92–1.16)	1.21 (1.04–1.32)	<0.0001	<0.0001	<0.0001
PTH	29.1 (23.5–38.9)	32.1 (24.3–47.5)	39.6 (27.5–55.9)	0.010	0.0092	<0.0001
CT	1.0 (0.5–1.6)	2.1 (0.8–3.6)	0.8 (0.5–2.4)	<0.0001	<0.0001	0.0036
BAP	11.5 (7.8–14.2)	15.0 (11.0–21.1)	26.2 (12.1–43.2)	<0.0001	<0.0001	<0.0001
tPINP	58.3 (41.1–69.9)	59.7 (40.1–98.5)	142.9 (115.0–173.1)	<0.0001	<0.0001	<0.0001
OPG	960.3 (582–1753)	1149 (380–1583)	1287 (300.2–1920.0)	0.010	0.020	0.0071
β-CTx	423.3 (275–615.3)	513.7 (356.6–708.8)	672.8 (422.5–952.8)	0.0073	<0.0001	<0.0001
NMID	13.3 (9.9–16.8)	14.1 (9.0–20.9)	15.4 (9.8–22.4)	0.0067	0.41	0.0036
FT3	4.4 (3.6–4.8)	4.3 (3.7–5.0)	4.1 (3.7–4.6)	0.58	0.0019	0.020
FT4	17.1 (16.2–17.9)	17.9 (15.7–19.6)	15.2 (11.7–18.8)	<0.0001	<0.0001	<0.0001
TSH	2.1 (1.3–3.1)	2.2 (1.4–3.6)	3.2 (2.1–4.1)	0.16	<0.0001	<0.0001
IL-6	14.3 (7.3–28.3)	31 (7.0–112.6)	34.7 (17.4–68.3)	<0.0001	<0.0001	<0.0001
PTHRP	124.7 (73–196.1)	244.6 (127.2–398.1)	300.9 (108.0–539.9)	<0.0001	<0.0001	<0.0001
K	4.0 (3.8–4.2)	4.0 (3.8–4.4)	3.9 (3.7–4.0)	0.13	<0.0001	0.020
Na	142 (141–143)	139 (137–141)	141 (139–143)	<0.0001	<0.0001	<0.0001
Mg	0.9 (0.80–0.96)	0.77 (0.65–0.85)	0.85 (0.80–0.90)	<0.0001	<0.0001	<0.0001
Cl	105 (104–107)	103 (101–105)	105 (104–107)	<0.0001	<0.0001	0.94

Note: Skewed distributed quantitative data were presented as median (P25, P75) and compared between groups using the Mann–Whitney U test. Count data were described as frequency (percentage %) and analyzed statistically using the chi-square test. BM: bone metastasis; NBM: none-bone metastasis; Ca: Calcium; P: Phosphorus; PTH: Parathyroid Hormone; CT: Calcitonin; BAP: Bone specific alkaline phosphatase; tP1NP: Total type I procollagen amino-terminal peptide; OPG: Ostoeprotegerin; NMID: N-Mid Osteocalcin; β-CTx: β-type I procollagen carboxy-terminal peptide; FT3: Free thiiodothyronine; FT4: Free thyroxine; TSH: Thyroid Stimulating Hormone; PTHRP: Parathyroid hormone-related protein; IL-6: Interleukin-6; K: Potassium; Na: Sodium; Mg: Magnesium; Cl: Chloridion. [a]P value for Healthy control vs. NBM. [b]P value for BM vs. NBM. [c]P value for Healthy control vs. BM.

Table 1: **The baseline Characteristics of each indicator.**

NBM), it was observed that the concentrations of serum Ca, P, PTH, tP1NP, β-CTx, OPG, BAP, IL-6, PTHRP, K, Na, and Mg were significantly higher in the bone metastasis group ($P < 0.05$). Conversely, the levels of FT3 and FT4 were significantly lower in the bone metastasis group compared to the non-bone metastasis group ($P < 0.05$). The analysis comparing the healthy control group and the non-bone metastasis group (Healthy control vs. NBM) showed statistically significant differences in all indicators, except for FT3, FT4, and K ($P < 0.05$). Additionally, the comparison between the healthy control group and the bone metastasis group (Healthy control vs. BM) revealed significant differences in all 18 serum indicators ($P < 0.05$), indicating a strong correlation between these serum indicators and the development of bone metastasis in NSCLC.

Variable selection

To enhance the practicality and operability of the model, multivariate logistic regression analysis was performed on a set of 20 independent variables (Supplementary Table S3) with the aim of eliminating redundant variables and identifying a more efficient, concise, and accurate set of variables. The findings revealed that out of the 20 variables, only 11 indicators were independent predictors for NSCLC bone metastasis. Specifically, K, FT4, CT, and BAP were identified as independent protective factors for NSCLC bone metastasis, while tP1NP, β-CTx, Ca, P, Na, Mg, and PTHRP were identified as independent risk factors for NSCLC bone metastasis (Fig. 2A).

To further control for confounding factors, Lasso regression analysis was employed for an in-depth selection of the 20 independent variables. By means of Lasso regression variable selection, a total of 13 independent variables were selected from the initial pool of 20, encompassing age, sex, tP1NP, Mg, K, P, Na, Ca, CT, FT4, PTHRP, BAP, and β-CTx. The findings demonstrated that the outcomes of feature selection derived from the Lasso regression analysis were congruent with those obtained from the multivariate logistic regression analysis. The analysis of multicollinearity for the 13 variables revealed a VIF value below 2, indicating the absence of significant multicollinearity concerns among the variables (Supplementary Table S4). Additionally, the application of Lasso regression feature selection and the examination of feature visualization using Shapley values (Fig. 2B and C) demonstrated that the top 13 primary features exhibited the highest predictive capacity.

Development and evaluation of the bone metastasis diagnostic model

In the model training, a positive class represented the presence of NSCLC bone metastasis, while a negative

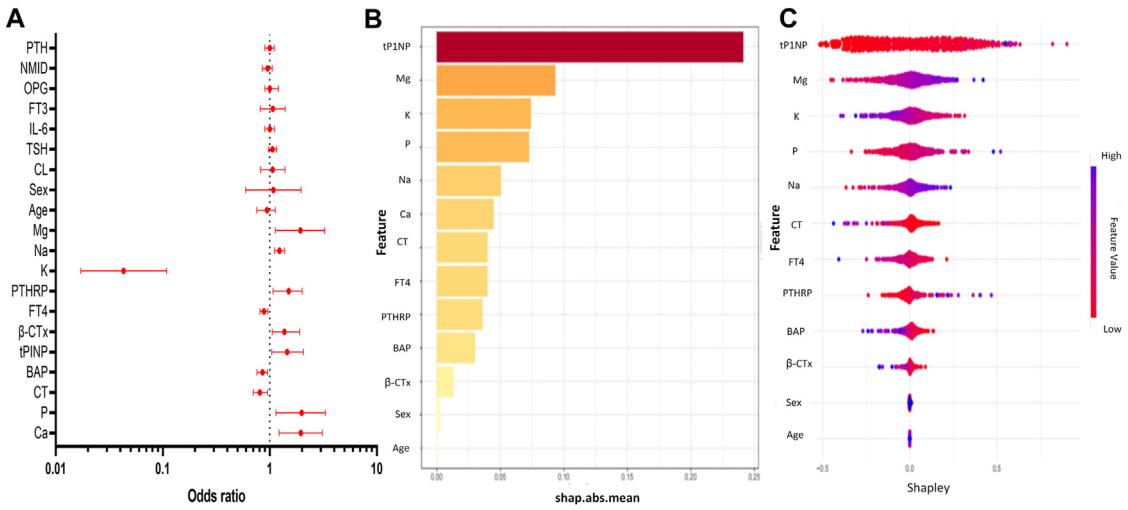

Fig. 2: Multivariate logistic regression analysis and variable selection process of Lasso regression. A) Multiple logistic regression analysis of the risk scores and clinical parameters. B and C) Feature visualization of Lasso regression feature factor analysis and Shapley value. Abbreviations: shay.abs.mean: Shapley additive explanations absolute mean value; Ca: Calcium; P: Phosphorus; PTH: Parathyroid Hormone; CT: Calcitonin; BAP: Bone specific alkaline phosphatase; tP1NP: Total type I procollagen amino-terminal peptide; OPG: Ostoeprotegerin; NMID: N-Mid Osteocalcin; β-CTx: β-type I procollagen carboxy-terminal peptide; FT3: Free thiiodothyronine; FT4: Free thyroxine; TSH: Thyroid Stimulating Hormone; PTHRP: Parathyroid hormone-related protein; IL-6: Interleukin-6; K: Potassium; Na: Sodium; Mg: Magnesium; Cl: Chloridion.

class represented the absence of bone metastasis. Following variable selection, the input data to train the model consisted of serum levels for 11 indicators closely related to the mechanism of lung cancer bone metastasis, in addition to age and sex of patients at admission. Utilizing these 13 features, we developed six different machine learning models, including DT, Logistic, MLP, RF, SVM, and Xgboost. The findings of this study demonstrate that the RF model displayed a significantly higher AUC value in comparison to other machine learning algorithms, within both the training and internal validation cohorts (Fig. 3A). Further examination of the data in the internal validation cohort revealed that the RF model exhibited an accuracy of 0.94, a sensitivity of 91.84%, a specificity of 94.12%, an F1 score of 0.92, and an AUC value of 0.98 (Fig. 3A, B, C, and Table 2). These outcomes strongly suggest that the RF model surpassed the other five models in terms of various performance parameters. Decision Curve Analysis (DCA) is a straightforward method to evaluate the clinical utility of disease diagnostic models. The DCA curve depicted in Fig. 3D further demonstrated that the RF model had the highest clinical utility.

External validation of the bone metastasis diagnostic model

This study involved conducting an external validation and performance comparison of six machine learning models using a cohort of 113 stage IV NSCLC patients from the Sixth People's Hospital Medical Alliance. Using a 5-fold cross-validation, it was observed that the AUC values for each model were similar, but the RF model had a significantly higher AUC value (Fig. 4A). In terms of predictive performance, the results obtained from the external validation cohort indicated that the RF model achieved an AUC of 0.97, followed by the Xgboost model with an AUC of 0.95, the SVM model with an AUC of 0.92, the MLP model with an AUC of 0.91, the Logistic model with an AUC of 0.90, and the DT model with an AUC of 0.79. Notably, regarding the results of the SPECT, the RF model consisting of clinical and plasma biomarkers can diagnose bone metastasis non-invasively yet reliably, as depicted in Fig. 4B. Furthermore, Table 3 provides an overview of the accuracy, AUC, kappa, sensitivity, specificity, Youden Index, and F1 Score of the six models in the external validation cohort. Data visualization was performed to assess the predictive performance of the six models on the external validation cohort. The calibration curve (Fig. 4C) demonstrated a satisfactory alignment between the predicted risk of the RF model and the observed risk. To summarize, the outcomes of the external confirm that the RF model demonstrates higher performance in the early prediction of bone metastasis (Fig. 4C).

Model interpretation

To ensure a comprehensive understanding of the selected variables, we employed the SHAP algorithm to highlight their predictive importance in the optimal RF model for bone metastasis. Fig. 5A visually demonstrates the 13 key features of the RF model, including

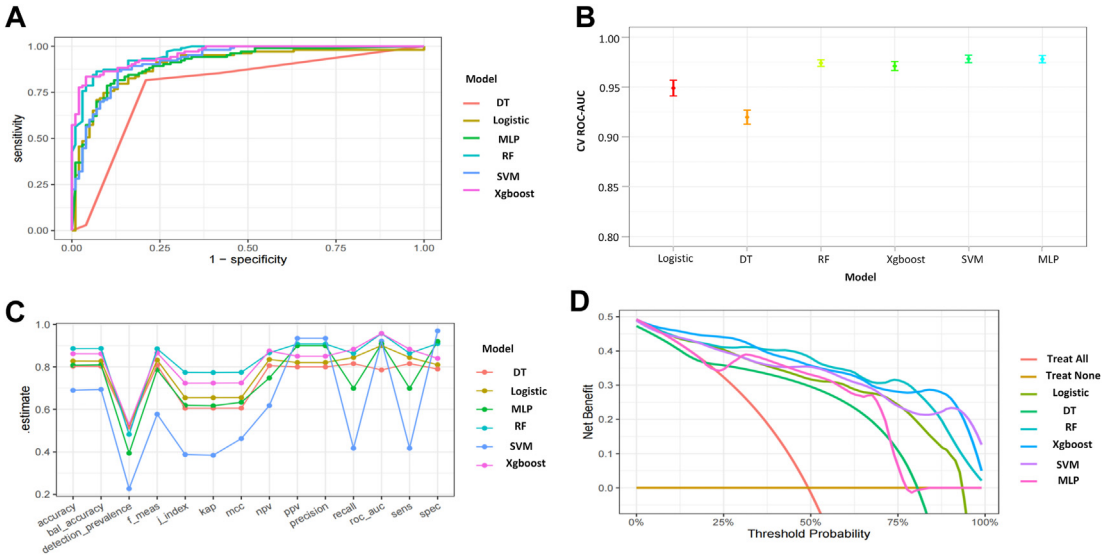

Fig. 3: Performance comparison of six models on the internal validation cohort. A) ROC curves for each model in the validation cohort; B) 95% confidence intervals for ROC-AUC obtained through cross-validation for each model; C) Parallel line graph of the evaluation metrics for each model; D) DCA curves for each model. Abbreviations: DT: Decision tree model; Logistic: Logistic regression model; MLP: Multilayer perceptron model; RF: Random forest model; SVM: Support vector machine model; Xgboost: Extreme gradient boosting model; f-means: F1 score; J-index: Youden index; kap: Kappa coefficient; mcc: Matthews correlation coefficient; NPV: Negative Predictive Value; PPV: Positive Predictive Value; CV ROC-AUC: cross-validation Area Under the Receiver Operating Characteristic Curve; Sens: Sensitivity; Spec: Specificity.

age, sex, and 11 serum indicators. The influence of each feature is illustrated by uniquely colored dots: red indicating higher risk values and blue indicating lower ones. Fig. 5B depicts the hierarchical organization of these 13 risk factors, underlining their significance in the model. The x-axis, representing SHAP values, indicates the importance of each factor. The strong link between the 11 serum indicators and the mechanism of bone metastasis in lung cancer suggests their value as dependable indicators for the clinically detecting this type of disease progression.

Prognostic value analysis and online computing platform for the model

To minimize evaluation bias, this study compared machine learning models with the clinically common SPECT imaging method. We included 316 NSCLC patients diagnosed without bone metastasis in a prospective validation analysis. The median time to SPECT examination in this cohort was 4.39 ± 1.15 months. During the follow-up, 123 patients developed bone metastasis, resulting in an incidence rate of 38.92%. The aim of this study was to assess the effectiveness of six models in detecting early-stage NSCLC bone metastasis using age, sex, and 11 serum indicators as inputs. Six models were used for prediction. Risk stratification was based on the models' predicted optimal cut-off value (average threshold for the six models = 40%). Patients were divided into low-risk or high-risk groups according to their risk probabilities relative to the cut-off value. The analysis of the match between predicted and actual cases of bone metastasis showed that the RF model had the highest predictive accuracy, as evidenced by a Kappa value of 0.87 (Table 4).

Model	Accuracy	AUC (95% CI)	Kappa	Sensitivity %	Specitivity %	Youden index	F1 score
DT	0.85	0.89 (0.82–0.93)	0.70	87.18%	82.35%	0.70	0.87
Logistic	0.69	0.80 (0.76–0.83)	0.37	87.76%	62.75%	0.51	0.88
MLP	0.67	0.71 (0.67–0.76)	0.17	42.86%	75.16%	0.18	0.43
RF	0.94	0.98 (0.95–0.99)	0.84	91.84%	94.12%	0.86	0.92
SVM	0.79	0.88 (0.81–0.94)	0.58	87.18%	70.59%	0.58	0.87
Xgboost	0.93	0.97 (0.93–0.99)	0.80	89.80%	93.46%	0.83	0.90

NSCLC: Non-Small Cell Lung Cancer; AUC: Area Under Curve; CI: Confidence Interval; DT: Decision tree model; Logistic: Logistic regression model; MLP: Multilayer perceptron model; RF: Random forest model; SVM: Support vector machine model; Xgboost: Extreme gradient boosting model.

Table 2: **Diagnostic performance of each model for NSCLC bone metastasis in internal validation cohort.**

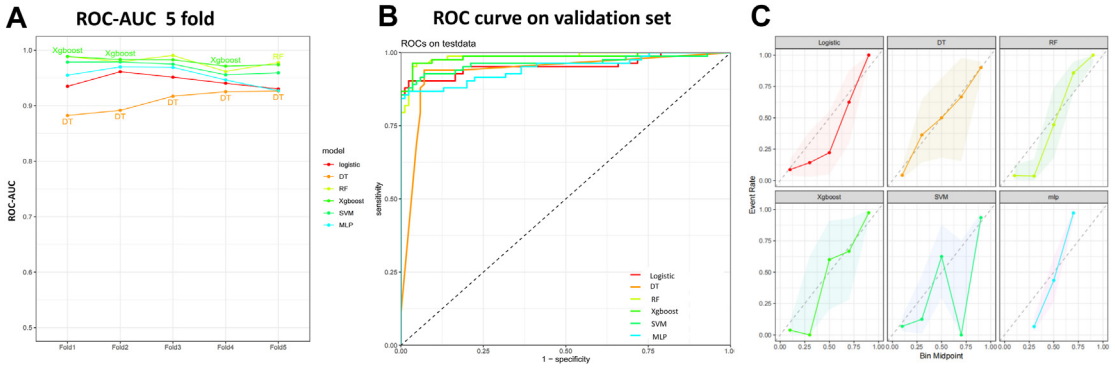

Fig. 4: Performance comparison of six models on the external validation cohort. A) ROC-AUC with 5-fold cross-validation; B) ROC curve on the validation cohort; C) Calibration plots (Reliability curve, dashed line represents perfectly calibrated) comparing the predictive performance of six models using external validation data from 113 cases. Abbreviations: DT: Decision tree model; Logistic: Logistic regression model; MLP: Multilayer perceptron model; RF: Random forest model; SVM: Support vector machine model; Xgboost: Extreme gradient boosting model; ROC-AUC: Area Under the Receiver Operating Characteristic Curve; ROC: Receiver Operating Characteristic Curve.

Further analysis, using the initial diagnostic data of NSCLC patients, showed that the optimal RF model provided a significant lead time of approximately 10.27 ± 3.58 months for predicting bone metastasis, according to the results of the SPECT (Table 4). For the prospective validation cohort, which progressed from no bone metastasis to developing bone metastasis, analysis of multiple test results indicated that the RF model's predictive values for patients who developed bone metastasis were significantly higher than those for patients who did not (Supplementary Fig. S4). This underscores the RF model's utility in monitoring disease progression. Additionally, Kaplan–Meier survival analysis showed that all six models predicted a higher probability of bone metastasis in the high-risk group (Fig. 6). Consequently, we created an online computing platform (https://bonemetastasis.shinyapps.io/shiny_cls_1model/) based on the optimal RF model (Fig. 7). This platform allows doctors and patients to perform calculations online.

Discussion

The oneset of bone metastasis is a significant poor prognostic risk factor for NSCLC patients,[2] and early clinical diagnosis and intervention are crucial for reducing the occurrence of SREs and improving patient quality of life. To identify high-risk individuals, this study incorporated age, sex, and 11 serum indicators related to bone metastasis into the model parameters. The first-ever Random Forest model based on blood biomarkers was developed for the early diagnosis and progression monitoring of NSCLC bone metastasis. Regarding the results of the SPECT, the RF model, which consists of clinical and plasma biomarkers, can diagnose bone metastasis non-invasively yet reliably. Additionally, the RF model could predict the occurrence of bone metastasis approximately 10.27 ± 3.58 months in advance. The findings of this study have the potential to predict bone metastasis occurrence in advance, facilitate prompt intervention, mitigate the occurrence of SREs, and ultimately enhance the prognosis of patients.

During the formation of bone metastasis, tumor cells settle in the bone and enter a dormant state. Upon stimulation by specific conditions, these dormant tumor cells become activated and start proliferating, leading to bone destruction and subsequent disruption of bone metabolism balance. During the transition from dormancy to activation, tumor cells release cytokines

Model	Accuracy	AUC (95% CI)	Kappa	Sensitivity %	Specitivity %	Youden index	F1 score
DT	0.80	0.79 (0.73–0.86)	0.61	81.93%	79.00%	0.61	0.81
Logistic	0.83	0.90 (0.85–0.94)	0.65	84.00%	81.00%	0.65	0.83
MLP	0.81	0.91 (0.86–0.95)	0.62	70.34%	91.76%	0.62	0.79
RF	0.89	0.97 (0.94–0.99)	0.77	86.11%	90.65%	0.77	0.89
SVM	0.69	0.92 (0.87–0.96)	0.38	42.36%	97.06%	0.39	0.58
Xgboost	0.86	0.95 (0.91–0.98)	0.72	88.36%	84.12%	0.72	0.87

NSCLC: Non-Small Cell Lung Cancer; AUC: Area Under Curve; CI: Confidence Interval; DT: Decision tree model; Logistic: Logistic regression model; MLP: Multilayer perceptron model; RF: Random forest model; SVM: Support vector machine model; Xgboost: Extreme gradient boosting model.

Table 3: **Diagnostic performance of each model for NSCLC bone metastases in external validation cohort.**

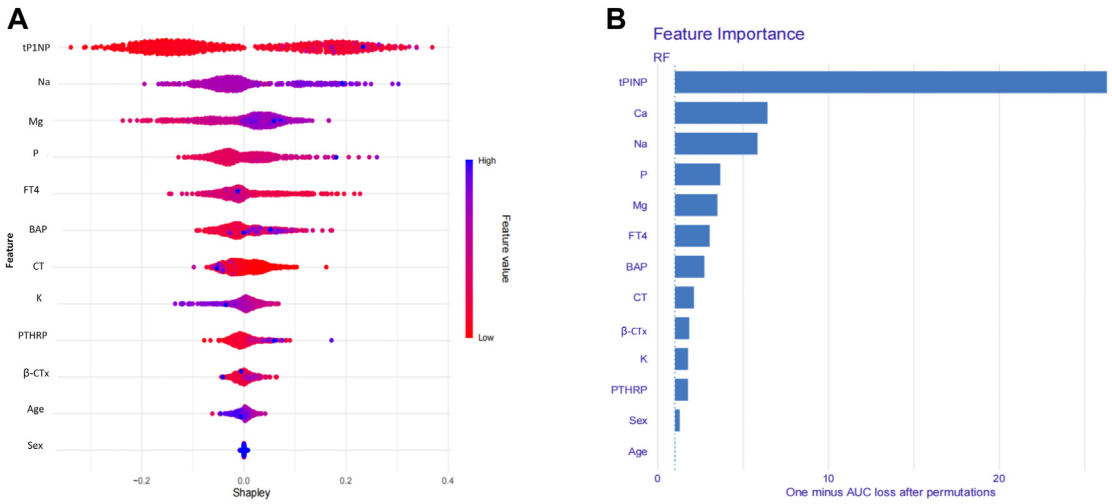

Fig. 5: RF model based on the SHAP algorithm. A) Feature attributes in the black-box model. Each line represents a feature, and the x-axis represents SHAP values, indicating the impact of the feature on the outcome. Each point represents a sample. The redder the colour, the larger the feature value; the bluer the colour, the smaller the feature value; B) Feature importance ranking indicated by SHAP. Abbreviations: AUC: Area Under the Curve; RF: Random forest; SHAP: Shapley additive explanations; Ca: Calcium; P: Phosphorus; CT: Calcitonin; BAP: Bone specific alkaline phosphatase; tP1NP: Total type I procollagen amino-terminal peptide; β-CTx: β-type I procollagen carboxy-terminal peptide; FT4: Free thyroxine; PTHRP: Parathyroid hormone-related protein; K: Potassium; Na: Sodium; Mg: Magnesium.

(such as OPG, PTHRP, and IL-6) to adapt to the bone microenvironment. Additionally, proliferating tumor cells release cytokines (such as IL-6, etc.), further promoting bone destruction. Thyroid-related hormones (FT3, FT4, TSH, PTH, and PTHRP) and calcitonin (CT) participate in regulating osteoclast generation, contributing to the modulation of bone metabolism balance.[15] When bone destruction reaches a certain level, disturbances in bone metabolism balance occur, leading to the release of bone metabolism-related molecules (including BAP, NMID, β-CTx, and tP1NP) into the bloodstream, resulting in electrolyte disturbances

Approaches	Patients n = 316	Predicted	Actual	Kappa	Actual (months)	*P* value
DT						<0.0001
Low risk (≤40.00%)	189	17.84%	17.46% (33/189)	0.71	9.76 ± 3.17	
High risk (>40.00%)	127	68.70%	70.87% (90/127)			
Logistic						<0.0001
Low risk (≤40.00%)	183	12.43%	12.57% (23/183)	0.81	9.53 ± 2.79	
High risk (>40.00%)	133	76.34%	75.19% (100/133)			
MLP						<0.0001
Low risk (≤40.00%)	189	11.35%	11.11% (21/189)	0.75	9.89 ± 2.96	
High risk (>40.00%)	127	77.86%	80.31% (102/127)			
RF						<0.0001
Low risk (≤40.00%)	192	14.05%	13.54% (26/192)	0.87	10.27 ± 3.58	
High risk (>40.00%)	124	74.05%	78.23% (97/124)			
SVM						<0.0001
Low risk (≤40.00%)	181	9.19%	9.39% (17/181)	0.79	9.57 ± 2.26	
High risk (>40.00%)	135	80.92%	78.51% (106/135)			
Xgboost						<0.0001
Low risk (≤40.00%)	195	12.43%	11.19% (23/195)	0.83	10.05 ± 3.64	
High risk (>40.00%)	121	76.34%	82.64% (100/121)			

AUC: Area Under Curve; CI: Confidence Interval; kappa: Kappa coefficient; DT: Decision tree model; Logistic: Logistic regression model; MLP: Multilayer perceptron model; RF: Random forest model; SVM: Support vector machine model; Xgboost: Extreme gradient boosting model.

Table 4: **Risk stratification based on the optimal cut-off value in the models.**

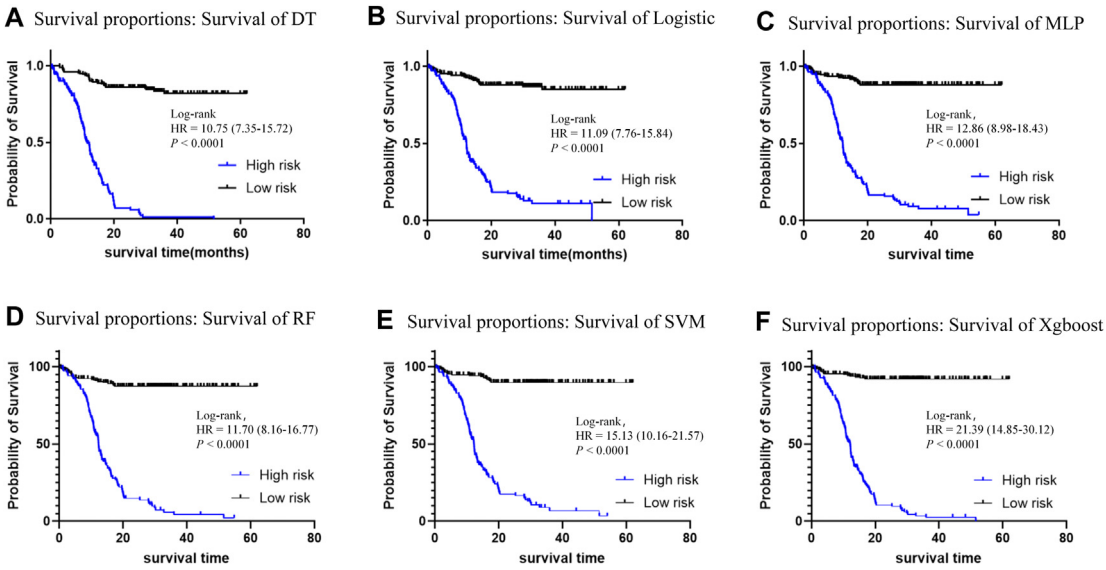

Fig. 6: Kaplan–Meier survival analysis of six models on the prospective validation cohort. A) DT: Decision tree model; B) Logistic: Logistic regression model; C) MLP: Multilayer perceptron model; D) RF: Random forest model; E) SVM: Support vector machine model; F) Xgboost: Extreme gradient boosting model. Abbreviations: HR: Hazard Ratio; Log-rank: Log–Rank test.

and exacerbating the occurrence of SREs.[12,14] Detecting these molecules can provide information about the early progression of tumor bone metastasis.

Considering the applicability of the model in clinical practice, this study selected relevant molecules for which corresponding reagents available for clinical testing. Due to the occurrence of bone metastasis being the result of multiple molecular interactions, the diagnostic efficacy of individual indicators for tumor bone metastasis is insufficient. Our findings also demonstrated that the diagnostic value of these individual indicators (AUC: 0.558–0.795) was limited, as illustrated in Supplementary Table S5. To improve precision, machine learning techniques were employed to evaluate age, sex, and 18 serum indicators associated with bone metastasis. Variable selection was conducted

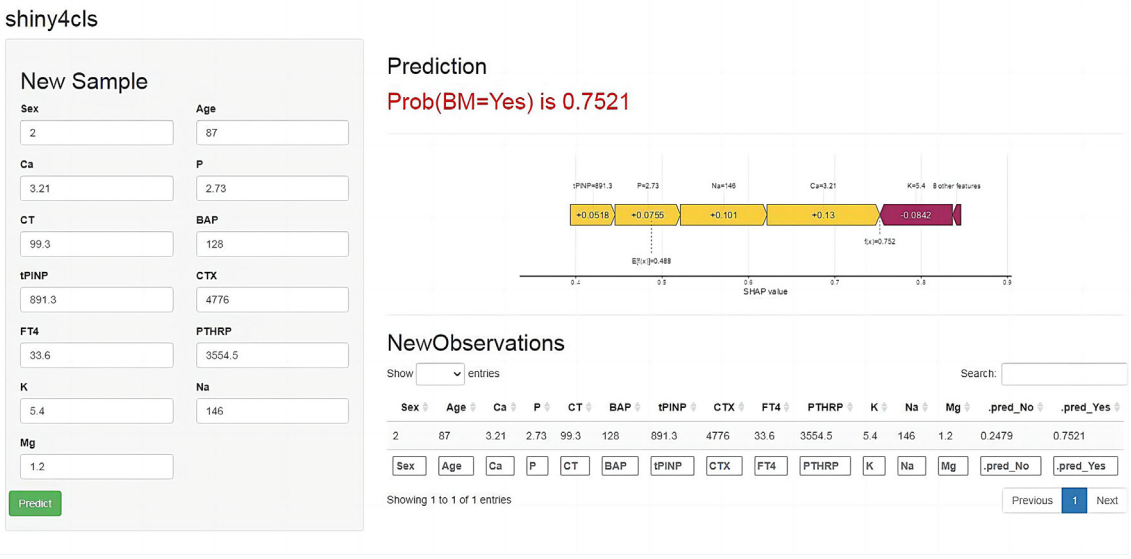

Fig. 7: Online computing platform presentation of the optimal RF model. Abbreviations: RF: Random forest; Ca: Calcium; P: Phosphorus; CT: Calcitonin; BAP: Bone specific alkaline phosphatase; tP1NP: Total type I procollagen amino-terminal peptide; CTx: β-type I procollagen carboxy-terminal peptide; FT4: Free thyroxine; PTHRP: Parathyroid hormone-related protein; K: Potassium; Na: Sodium; Mg: Magnesium; SHAP value: Shapley additive explanations absolute mean value; Pred: Prediction; Prob: Probability; BM: bone metastasis.

among 664 patients in the derivation cohort, consisting of 597 cases of adenocarcinoma and 67 cases of squamous cell carcinoma. It was determined that variables such as pathological classification did not meet the criteria for inclusion in the multivariate logistic regression analysis and were therefore excluded from the study. Subsequent ROC curve analysis indicated that there was no statistically significant disparity in the diagnostic efficacy of the RF model between the adenocarcinoma and squamous carcinoma groups within the derivation cohort (Supplementary Fig. S5). Through feature selection using multivariate logistic regression analysis and LASSO regression analysis, 11 serum indicators were selected in addition to age and sex, which were used as input parameters for the machine learning model.

This study employed six widely-used machine learning algorithms on medical data to develop a diagnostic model for bone metastasis in NSCLC.[18–20] The findings revealed that the RF model exhibited higher performance compared to the other models in accurately diagnosing bone metastasis, as demonstrated in both the training and the internal validation cohorts. In Fig. 3D, the decision curve analysis (DCA) of the six models also demonstrated that the RF model exhibited higher clinical utility. This study also found that three models (MLP, DT, and Logistic) had portions of their DCA curves below the bottom line, indicating poor performance of these models at the decision thresholds, resulting in a decline in the curve within this range. Furthermore, external validation substantiated the model's effectiveness, surpassing the other models with an AUC of 0.93. Prospective validation further supported the RF model's superiority in the timely detection and prognosis of bone metastasis in NSCLC. Regarding the results of the SPECT, the RF model could predict the occurrence of bone metastasis approximately 10.27 ± 3.58 months in advance. These consistent findings may improve doctors' confidence in using predictive models. The RF algorithm's outstanding performance aligns with prior research, as the use of RF excels in serum-based diagnostic models.[21,22] Its integration of decision trees and feature synthesis enhances accuracy,[23–25] which is suitable for the multi-stage, multi-step nature of tumor bone metastasis mechanisms.

The interpretability of medical diagnostic models is crucial for doctor acceptance and trust. We collected relevant serum indicators, such as cytokines,[7,9,11] blood calcium,[22] phosphorus,[26,27] electrolytes,[23] hormones, and bone turnover markers,[28–30] to ensure the relevance of model parameters to diagnostic outcomes in the complex bone metastasis process. SHAP value analysis was used to assess model interpretability, with the corresponding SHAP values shown in Supplementary Fig. S1 and the feature importance rankings shown in Supplementary Fig. S2. Additionally, Supplementary Fig. S3 describes the computation process for individual cases in the six models, aiding doctors in understanding how the models make predictions. To assess the model's robustness, we reported the missing rates for each variable among 37 patients (Supplementary Table S6). We found that the age and sex distribution of these patients closely matches that of the derivation cohort, suggesting the data are missing at random. We utilized a multiple imputation method based on random forests to address the missing values. The sensitivity analysis within the internal validation cohort, detailed in Supplementary Table S7, confirmed the optimal RF model's robustness post-imputation within the internal validation cohort. This consistency in performance, even with missing data addressed, underscores the RF model's reliability for practical use. In summary, the RF model in this study offers high interpretability and informs doctors about how model predictions were made. To benefit a broader audience and validate the model, an online computing platform based on the optimal RF model was developed. It assists clinical doctors in the early diagnosis of NSCLC bone metastasis, addressing current challenges posed by the onset of bone metastasis.

The innovation of this study can be highlighted in two main aspects. Firstly, it considers serum indicators throughout the entire bone metastasis process and establishes an interpretable machine learning model, enhancing model understanding for users. Secondly, it introduces a simple, accurate, and continuous bone metastasis prediction tool, expected to identify risk months ahead of imaging techniques. However, certain limitations exist in this study. Molecular imaging based on PET-CT can detect bone metastasis earlier than SPECT imaging. The results of this study lay the foundation for future research in fusion imaging based on PET-CT. In addition, incorporating information on patients' molecular genetic factors and driver gene mutations may be helpful to expand the scope and effectiveness of the model. The dataset primarily comprises NSCLC patients suspected of having bone metastasis, thereby rendering the model more appropriate for this particular patient population. Its generalizability to other solid tumor bone metastasis remains uncertain. Future research efforts will seek to validate this model on a broader scope by incorporating supplementary parameters related to bone metastasis, thereby enhancing its adaptability and applicability as the database evolves.

In conclusion, the RF model developed in this study has the potential to serve as an auxiliary tool for the early diagnosis and prognostic assessment of bone metastasis in NSCLC patients. Regarding the results of the SPECT, the RF model demonstrates a high level of sensitivity in accurately diagnosing bone metastasis. Additionally, an online computing platform was developed for the prediction of bone metastasis in NSCLC, presenting a novel approach with the potential to improve the early

screening for bone metastasis and prognostic assessment of NSCLC patients.

Contributors

Teng Xiaoyan: Conceptualization (Equal), Formal analysis (Lead), Data curation (Supporting), Funding acquisition (Equal), Writing original draft (Lead). Han Kun: Data curation (Lead), Investigation (Supporting). Jin Wei: Data curation (Supporting), Investigation (Supporting). Ma Liru: Data curation (Supporting), Investigation (Supporting). Lirong Wei: Data curation (Supporting), Investigation (Supporting). Daliu Min: Conceptualization (Supporting), Project administration (Supporting). Libo Chen: Conceptualization (Supporting), Project administration (Supporting). Du Yuzhen: Conceptualization (Lead), Funding acquisition (Equal), Project administration (Lead). All authors read and approved the final manuscript.

Data sharing statement

We are unable to provide access to our dataset for privacy reasons. The protocol and statistical analysis methods used in the study can be requested directly from the corresponding author after approval.

Declaration of interests

All authors declare no competing interests.

Acknowledgements

None.

Appendix A. Supplementary data

Supplementary data related to this article can be found at https://doi.org/10.1016/j.eclinm.2024.102617.

References

1 Adams SJ, Stone E, Baldwin DR, Vliegenthart R, Lee P, Fintelmann FJ. Lung cancer screening. *Lancet*. 2023;401(10374):390–408. https://doi.org/10.1016/S0140-6736(22)01694-4.
2 Jung JM, Hyun SJ, Kim KJ. Surgical impacts of metastatic non-small cell lung cancer to the thoracic and lumbar spine. *J Korean Med Sci*. 2021;36(7):e52. https://doi.org/10.3346/jkms.2021.36.e52.
3 Wu B, Wei S, Tian J, Song X, Hu P, Cui Y. Comparison of the survival time in the non-small cell lung cancer patients with different organ metastasis. *Chin J Lung Cancer*. 2019;22(2):105–110. https://doi.org/10.3779/j.issn.1009-3419.2019.02.05.
4 Xu Y, Zhang C, Guo X, Liu L, Han X, Wang G. The clinical feature of bone metastases in lung cancer patients with different pathological types. *Chinese J Orthop*. 2019;39(6):329–335. https://doi.org/10.3760/cma.j.issn.0253-2352.2019.06.002.
5 Fornetti J, Welm AL, Stewart SA. Understanding the bone in cancer metastasis. *J Bone Miner Res*. 2018;33(12):2099–2113. https://doi.org/10.1002/jbmr.3618.
6 Wood SL, Brown JE. Skeletal metastasis in renal cell carcinoma: current and future management options. *Cancer Treat Rev*. 2012;38(4):284–291. https://doi.org/10.1016/j.ctrv.2011.06.011.
7 Peterson LM, O'Sullivan J, Wu QV, et al. Prospective study of serial (18) F-FDG PET and (18)F-fluoride PET to predict time to skeletal-related events, time to progression, and survival in patients with bone-dominant metastatic breast cancer. *J Nucl Med*. 2018;59(12):1823–1830. https://doi.org/10.2967/jnumed.118.211102.
8 Zhang C, Mao M, Guo X, et al. Nomogram based on homogeneous and heterogeneous associated factors for predicting bone metastases in patients with different histological types of lung cancer. *BMC Cancer*. 2019;19(1):238. https://doi.org/10.1186/s12885-019-5445-3.
9 Wood DE, Kazerooni EA, Baum SL, et al. Lung cancer screening, version 3.2018, NCCN clinical practice guidelines in oncology. *J Natl Compr Canc Netw*. 2018;16(4):412–441. https://doi.org/10.6004/jnccn.2018.0020.
10 Roodman GD. Mechanisms of bone metastasis. *N Engl J Med*. 2004;350(16):1655–1664. https://doi.org/10.1056/NEJMra030831.
11 Coleman RE, Croucher PI, Padhani AR, et al. Bone metastases. *Nat Rev Dis Primers*. 2020;6(1):83. https://doi.org/10.1038/s41572-020-00216-3.
12 Wang M, Xia F, Wei Y, Wei X. Molecular mechanisms and clinical management of cancer bone metastasis. *Bone Res*. 2020;8(1):30. https://doi.org/10.1038/s41413-020-00105-1.
13 Muscarella AM, Aguirre S, Hao X, Waldvogel SM, Zhang XH. Exploiting bone niches: progression of disseminated tumor cells to metastasis. *J Clin Invest*. 2021;131(6):e143764. https://doi.org/10.1172/JCI143764.
14 Clezardin P, Coleman R, Puppo M, et al. Bone metastasis: mechanisms, therapies, and biomarkers. *Physiol Rev*. 2021;101(3):797–855. https://doi.org/10.1152/physrev.00012.2019.
15 Chung JH, Park MS, Kim YS, et al. Usefulness of bone metabolic markers in the diagnosis of bone metastasis from lung cancer. *Yonsei Med J*. 2005;46(3):388–393. https://doi.org/10.3349/ymj.2005.46.3.388.
16 Deo RC. Machine learning in medicine. *Circulation*. 2015;132(20):1920–1930. https://doi.org/10.1161/CIRCULATIONAHA.115.001593.
17 Youth Specialists Committee of Lung Cancer, Beijing Medical Award Foundaton, Chinese Lung Cancer Union. Expert Consensus on the diagnosis and treatment of bone metastasis in lung cancer (2019 version). *Chin J Lung Cancer*. 2019;4(22):187–207. https://doi.org/10.3779/j.issn.1009-3419.2019.04.01.
18 Goecks J, Jalili V, Heiser LM, Gray JW. How machine learning will transform biomedicine. *Cell*. 2020;181(1):92–101. https://doi.org/10.1016/j.cell.2020.03.022.
19 Shilo S, Rossman H, Segal E. Axes of a revolution: challenges and promises of big data in healthcare. *Nat Med*. 2020;26(1):29–38. https://doi.org/10.1038/s41591-019-0727-5.
20 Hong S, Youk T, Lee SJ, Kim KM, Vajdic CM. Bone metastasis and skeletal-related events in patients with solid cancer: a Korean nationwide health insurance database study. *PLoS One*. 2020;15(7):e0234927. https://doi.org/10.1371/journal.pone.0234927.
21 Truslow JG, Goto S, Homilius M, et al. Cardiovascular risk assessment using artificial intelligence-enabled event adjudication and hematologic predictors. *Circ Cardiovasc Qual Outcomes*. 2022;15(6):e008007. https://doi.org/10.1161/CIRCOUTCOMES.121.008007.
22 Chen QY, Que SJ, Chen JY, et al. Development and validation of metabolic scoring to individually predict prognosis and monitor recurrence early in gastric cancer: a large-sample analysis. *Eur J Surg Oncol*. 2022;48(10):2149–2158. https://doi.org/10.1016/j.ejso.2022.06.019.
23 Liu WC, Li MX, Qian WX, et al. Application of machine learning techniques to predict bone metastasis in patients with prostate cancer. *Cancer Manag Res*. 2021;13:8723–8736. https://doi.org/10.2147/CMAR.S330591.
24 Ogunleye A, Wang QG. XGBoost model for chronic kidney disease diagnosis. *IEEE/ACM Trans Comput Biol Bioinform*. 2020;17(6):2131–2140. https://doi.org/10.1109/TCBB.2019.2911071.
25 Guan X, Zhang B, Fu M, et al. Clinical and inflammatory features based machine learning model for fatal risk prediction of hospitalized COVID-19 patients: results from a retrospective cohort study. *Ann Med*. 2021;53(1):257–266. https://doi.org/10.1080/07853890.2020.1868564.
26 Wang H, Tian L, Liu J, et al. The osteogenic niche is a calcium reservoir of bone micrometastases and confers unexpected therapeutic vulnerability. *Cancer Cell*. 2018;34(5):823–839.e7. https://doi.org/10.1016/j.ccell.2018.10.002.
27 Zhu Z, Yang G, Pang Z, Liang J, Wang W, Zhou Y. Establishment of a regression model of bone metabolism markers for the diagnosis of bone metastases in lung cancer. *World J Surg Oncol*. 2021;19(1):27. https://doi.org/10.1186/s12957-021-02141-5.
28 Li R, Zhu X, Zhang M, Zong G, Zhang K. Association of serum periostin level with classical bone turnover markers and bone mineral density in Shanghai Chinese postmenopausal women with osteoporosis. *Int J Gen Med*. 2021;14:7639–7646. https://doi.org/10.2147/IJGM.S335296. eCollection 2021.
29 Teng X, Wei L, Han L, Min D, Du Y. Establishment of a serological molecular model for the early diagnosis and progression monitoring of bone metastasis in lung cancer. *BMC Cancer*. 2020;20(1):562. https://doi.org/10.1186/s12885-020-07046-2.
30 Tang C, Liu Y, Qin H, et al. Clinical significance of serum BAP, TRACP 5b and ICTP as bone metabolic markers for bone metastasis screening in lung cancer patients. *Clin Chim Acta*. 2013;426:102–107. https://doi.org/10.1016/j.cca.2013.09.011.